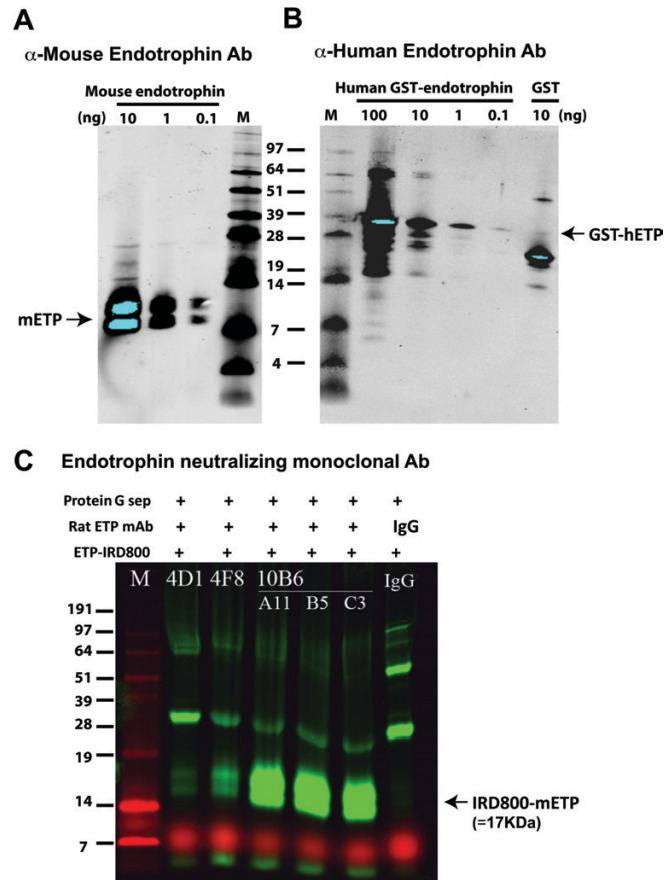


## Supplemental Information

### Adipocyte-derived endotrophin promotes malignant tumor progression

Jiyoung Park<sup>1</sup>, and Philipp E. Scherer<sup>1,2,3\*</sup>

<sup>1</sup>Touchstone Diabetes Center, Departments of Internal Medicine and <sup>2</sup>Cell Biology and <sup>3</sup>Simmons Cancer Center, The University of Texas Southwestern Medical Center, Dallas, Texas 75390, USA.



**Figure S1. Generation of endotrophin-specific antibodies.** **A.** HEK-293 cell produced mouse endotrophin was subjected to Western blotting using rabbit anti-mouse endotrophin polyclonal antibody. **B.** Bacterially produced GST-fused recombinant human endotrophin protein was subjected to western blotting using a rabbit anti-human endotrophin polyclonal antibody. GST protein was used as a negative control. The arrow points at endotrophin. **C.** Rat anti-mouse endotrophin monoclonal antibodies efficiently capture the native form of endotrophin protein. IRD (infrared dye)-800 labeled native form of endotrophin protein was incubated with either endotrophin monoclonal antibodies, including 4D1, 4F8, 10B6-A11, 10B6-B5, and 10B6-C3 or a rat-IgG for 2 hours at room temperature and subsequently incubated with Protein G Sepharose for 1 hour. The protein-Sepharose complex was separated on a 10-20 % Tricine gel after 3 times washing with PBS. Captured endotrophin protein was visualized on a Licor Odyssey Infrared Scanner (Licor Bioscience). Green color represents the IRD800 channel.

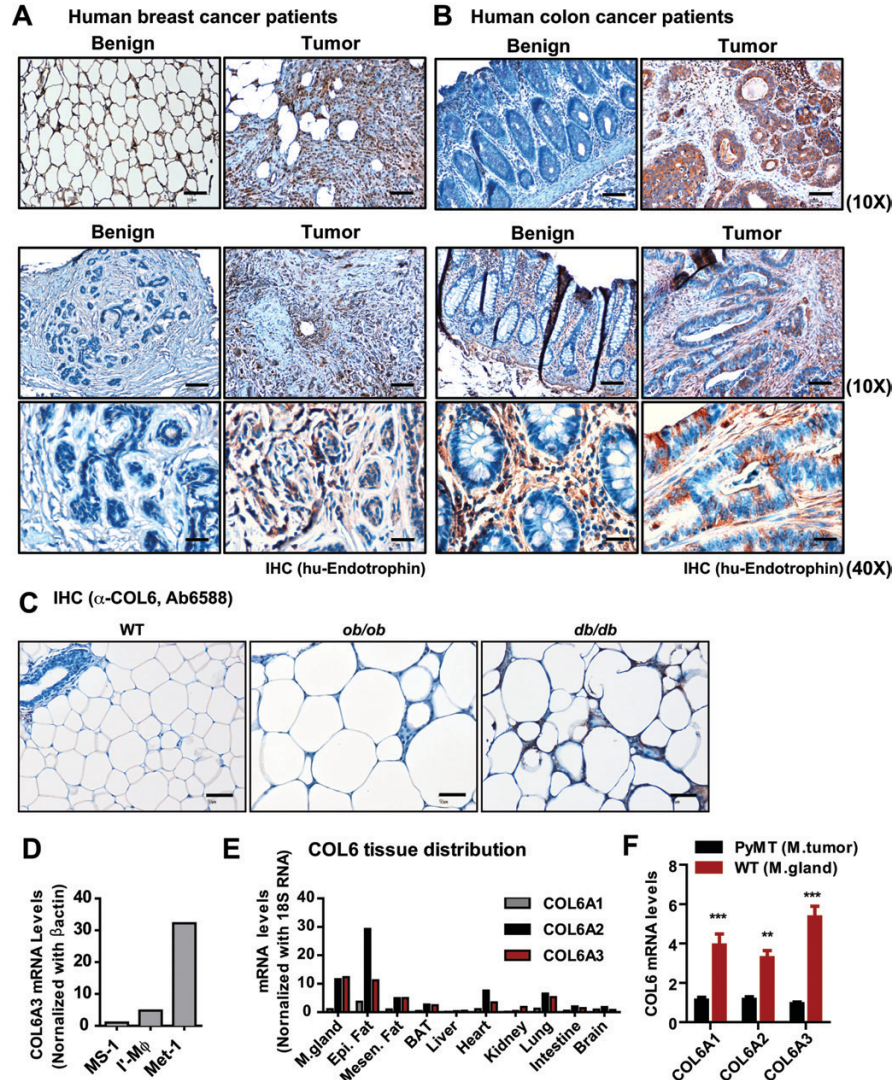


**Figure S2. Endotrophin expression levels in various tissues.** A-B. Endotrophin is highly expressed in human breast cancer (A) and colon cancer (B) tissues compared to samples obtained from benign lesions. Human breast and colon cancer samples (UTSW Medical Cancer Human Tissue Bank) were immunostained with polyclonal human endotrophin antibodies (TX933). Human samples for breast- and colon cancer patients were analyzed. Scale bars: 100  $\mu$ m (10 $\times$ ) and 25  $\mu$ m (40 $\times$ ). C. COL6 immunostaining for adipose tissues of obese animals such as *ob/ob* and *db/db* mice compared to lean control mice (pan-collagen 6 antibody, Abcam, Ab6588). Scale bars: 50 $\mu$ m. D. Endotrophin mRNA levels in various cell lines: mRNA levels for endotrophin were determined by qRT-PCR with various cell lines such as MS1 (mouse endothelial cells), mouse primary macrophages, and Met-1 (mouse mammary cancer cells). qRT-PCR results were normalized with  $\beta$ -actin. E-F. Tissue distribution of COL6. Various tissues were collected from 10-week-old FVB WT mice or tumor tissues from PyMT mice and analyzed for COL6A1, -A2, and -A3 mRNA levels. qRT-PCR results were normalized with 18S RNA (E). \*\* $p < 0.01$ , \*\*\* $p < 0.001$  vs. mammary gland (M. gland) by 2-way ANOVA ( $n = 4$  /group). Results were normalized with  $\beta$ -actin and represented as mean  $\pm$  SEM (F).

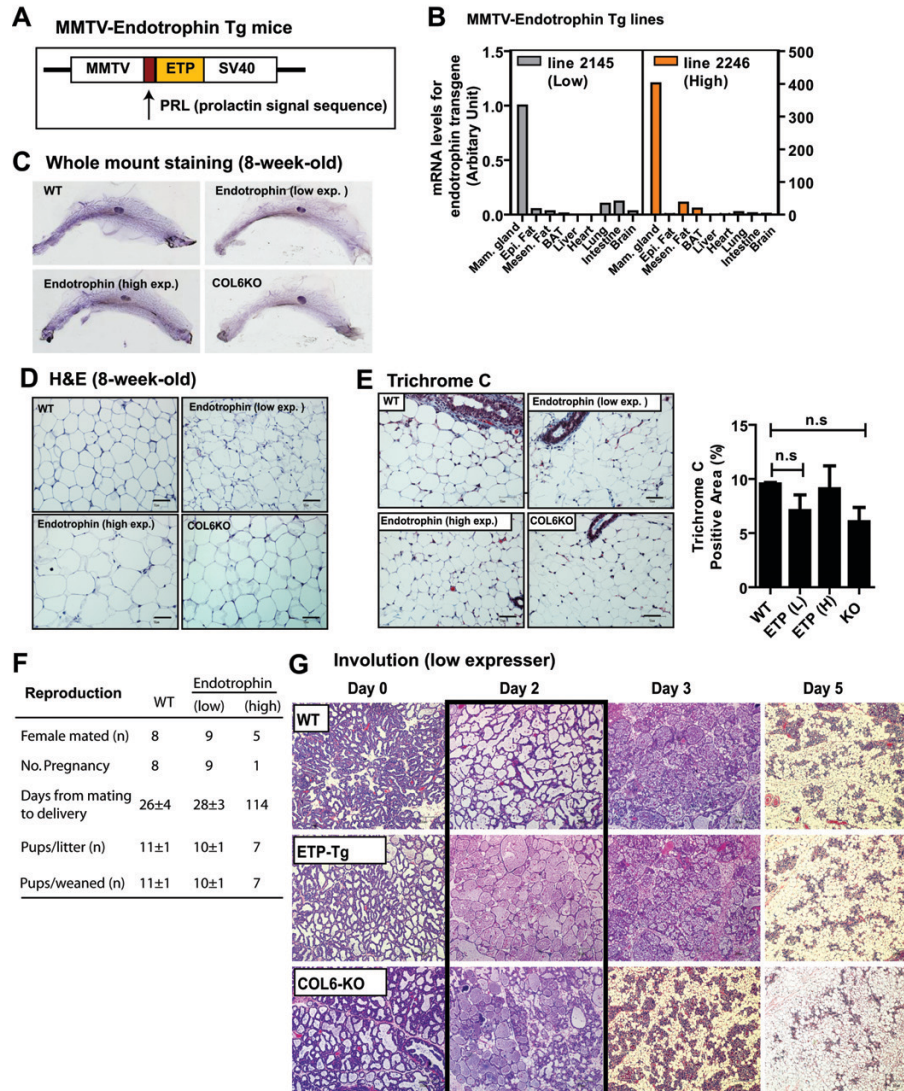


**Figure S3. Generation of the MMTV-endotrophin transgenic mice.** **A.** Diagram for the MMTV-endotrophin transgenic mice. **B.** Tissue distributions of endotrophin transgene. mRNA levels for the endotrophin transgene were determined by qRT-PCR with various tissues from low expressers (line 2145, left Y-axis) and high expressers (line 2246, right Y-axis). Results were normalized with  $\beta$ -actin. **C-D.** Mammary ductal epithelium growth develops normally in the endotrophin transgenic mice. Morphological analysis of ductal epithelial growth was performed with whole mount preparations (**C**) and H&E stain (**D**) of inguinal mammary glands from 8-week-old WT, endotrophin transgenic (ETP-Tg; low and high expresser), and COL6A1<sup>-/-</sup> (COL6KO) mice. Scale bars: 50  $\mu$ m in H&E. **E.** Tissue fibrosis was determined by Masson's Trichrome C staining of 8-week-old mice. Collagen fibrils are stained with blue. Scale bars: 50  $\mu$ m. Quantified results are represented as mean  $\pm$  SEM (n=5/ group). p=n.s (no significance) vs. WT by *unpaired t-test*. **F.** Reproduction was determined by measuring pregnancy incidence, litter size, and duration of pregnancy (from mating to delivery). n=5-9 per group. **G.** The rate of involution was determined by morphological analysis with H&E preparations of mammary gland at indicated days after forced weaning.



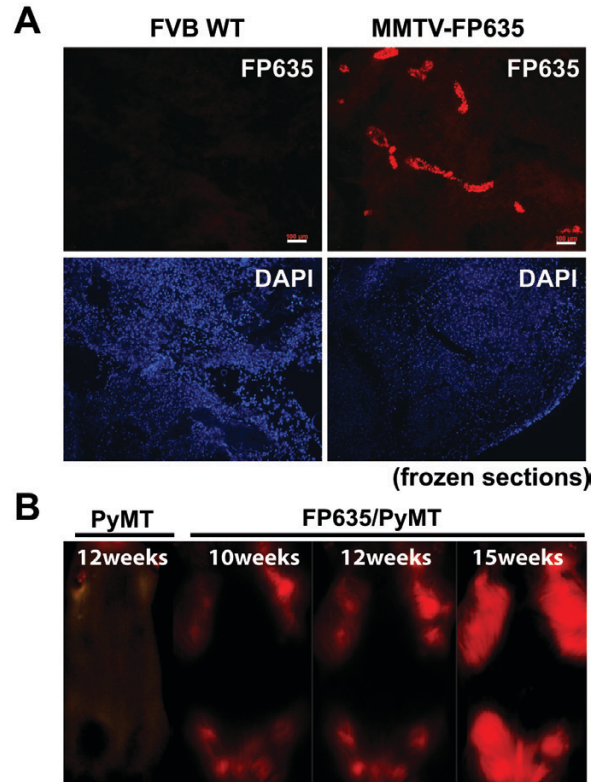


**Figure S4. Quantification of tumor progression with the infrared-fluorescence protein (FP635) transgenic mice driven by MMTV promoter.** **A.** Infrared fluorescence protein (FP635) is exclusively expressed in the mammary ductal epithelium under the control of MMTV promoter. We have established a MMTV-FP635 transgenic mouse line starting with 7 independent founders by screening for FP635 fluorescence protein expression in frozen sectioned mammary gland tissues. Images were acquired using a Leica confocal microscope. The DAPI stain highlights nuclei. **B.** Longitudinal whole body in vivo tumor imaging with MMTV-FP635 transgenic mice (FP635/PyMT). Female MMTV-FP635 mice were crossed with male MMTV-PyMT mice to obtain female FP635/PyMT mice. Tumor volume for the PyMT/FP635 mice at indicated time points was determined by integration of infrared fluorescence signal expressed in the ductal epithelium during tumor progression. Images were acquired with a Maestro Fluorescence Scanner.

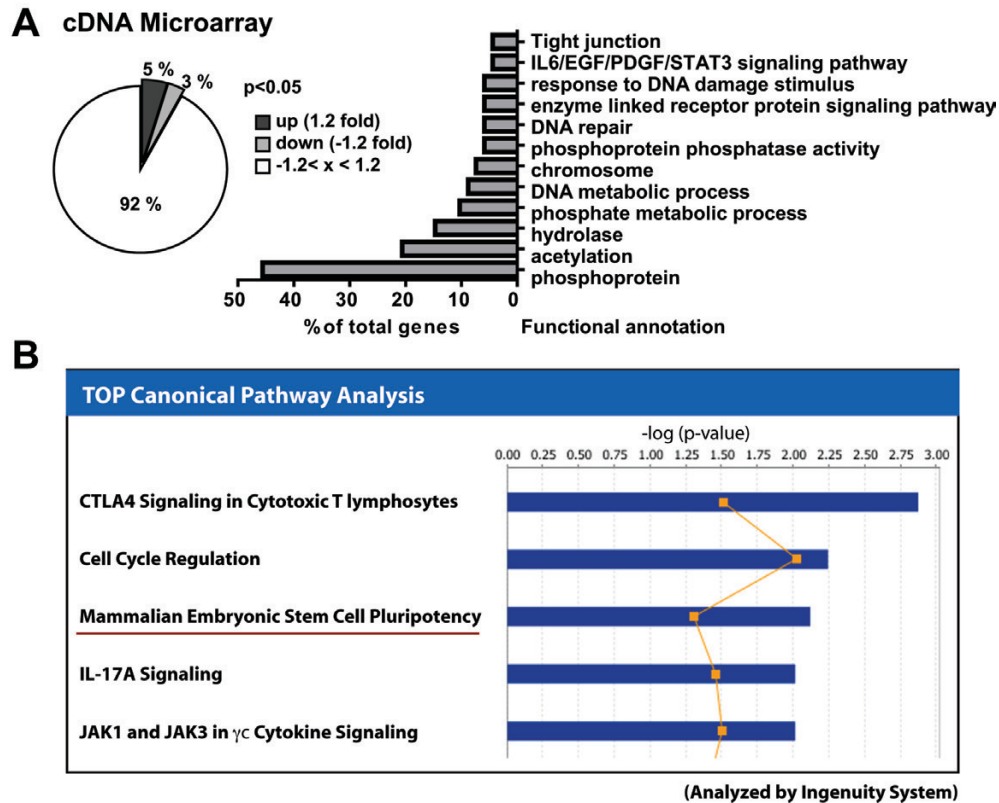


**Figure S5. Gene expression profiling for tumor tissues from PyMT/endotrophin compared to PyMT.**  
**A.** cDNA microarrays for tumor tissues from PyMT vs. PyMT/ETP were analyzed. Diagram represents % of modulated genes by PyMT/ETP vs. PyMT. Functional annotation for genes significantly changed by endotrophin is represented as a bar-graph. Analysis was performed with DAVID Bioinformatics Resources 6.7, National Institute of Allergy and Infectious Diseases (NIAID), NIH (<http://david.abcc.ncifcrf.gov/home.jsp>). **B.** Canonical pathway analysis for the cDNA microarray data was performed with Ingenuity System (<http://www.ingenuity.com>). Top 5 ranked canonical pathways are represented as a bar graph.

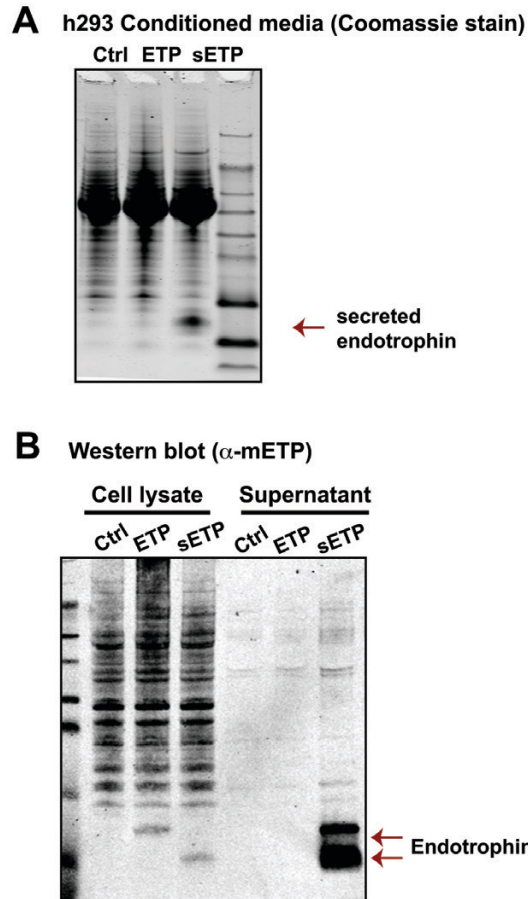


**Figure S6. Generation of mammalian cell-produced endotrophin.** Mouse endotrophin cDNA in the presence of either a 5' in-frame prolactin signal sequence (sETP) or an adiponectin signal sequence (ETP) was cloned into the mammalian expression vector pRA-GFP. Each construct was transiently transfected into HEK293 cells and supernatants were collected 2 days post transfection. **A.** Supernatants were subjected to SDS-PAGE and Coomassie staining to check for endotrophin secretion. **B.** Cell lysates and supernatants were subjected to western blotting with anti-mouse endotrophin antibody. Intracellular endotrophin was presented in both ETP- and sETP-expressing cells. Whereas only sETP-overexpressing cells secrete endotrophin into the media, since the adiponectin signal sequence is an inefficient signal for secretion of a passenger protein. Arrow indicates secreted endotrophin.

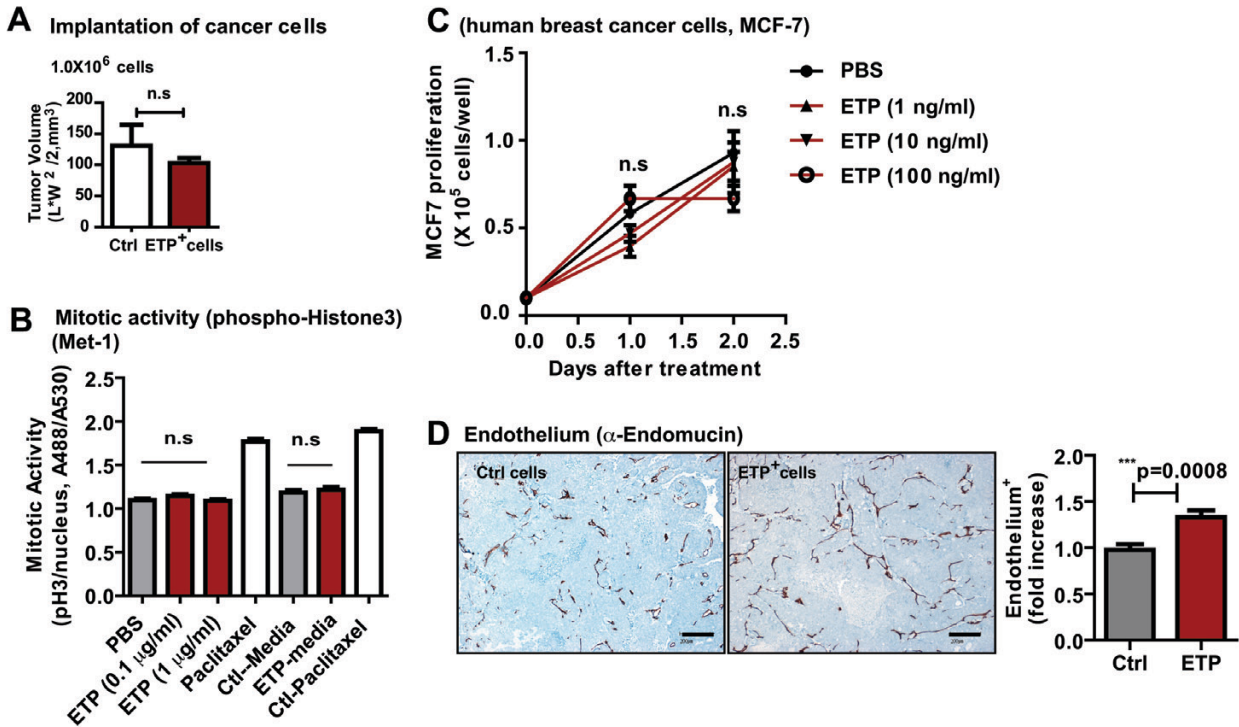


**Figure S7. Endotrophin has a limited effect on tumor cell proliferation.** **A.** Endotrophin<sup>+</sup>-cancer cells grow at comparable rates as ctrl-cancer cells. An equal number of cancer cells were freshly isolated from tumor tissues of PyMT (ctrl-cancer cells) and PyMT/endotrophin (ETP<sup>+</sup>-cancer cells) and implanted into WT mice (1 × 10<sup>6</sup> cells/ mouse). Tumor volume was determined 1 month post-implantation. Quantitative results are represented as mean ± SEM (n=7/ group). p=n.s vs. Ctrl-cancer cells by *unpaired t-test*. **B.** Met-1 cells were seeded into the 96 well plates and incubated with DMEM/10% FBS/PBS, DMEM/10% FBS/endotrophin, or conditioned media acquired from HEK293 or HEK293/endotrophin-overexpressing cells for 24 hours. Mitotic activity was measured with a Mitotic Index Assay Kit (Active Motif) following the manufacturer's protocol. Paclitaxel (1 μM) was used as a positive control of mitosis. Quantified results are represented as mean ± SEM (n=10/group) p=n.s vs. PBS or Ctrl-media by *unpaired t-test*. **C.** Human breast cancer cells, MCF7 (0.1 × 10<sup>5</sup>) were plated in the 24 well plates with or without recombinant endotrophin protein and cell numbers were counted over time. The quantification of results is represented as mean ± SEM (n=6/group, triplicate). p=n.s vs. PBS by *unpaired t-test*. **D.** Tumor tissues taken from Fig. 7A were immunostained for endothelium with anti-endomucin antibody (Santa Cruz. Biotechnology, Inc., sc-65495), demonstrating that the vascularization is significantly increased in ETP<sup>+</sup>-cancer cells compared to Ctrl-cancer cells. Endomucin positive area was quantified and represented as mean ± SEM (multiple images, n=4/group). \*\*\*p=0.0008 vs. ctrl by *unpaired t-test*. Scale bars: 200 μm.



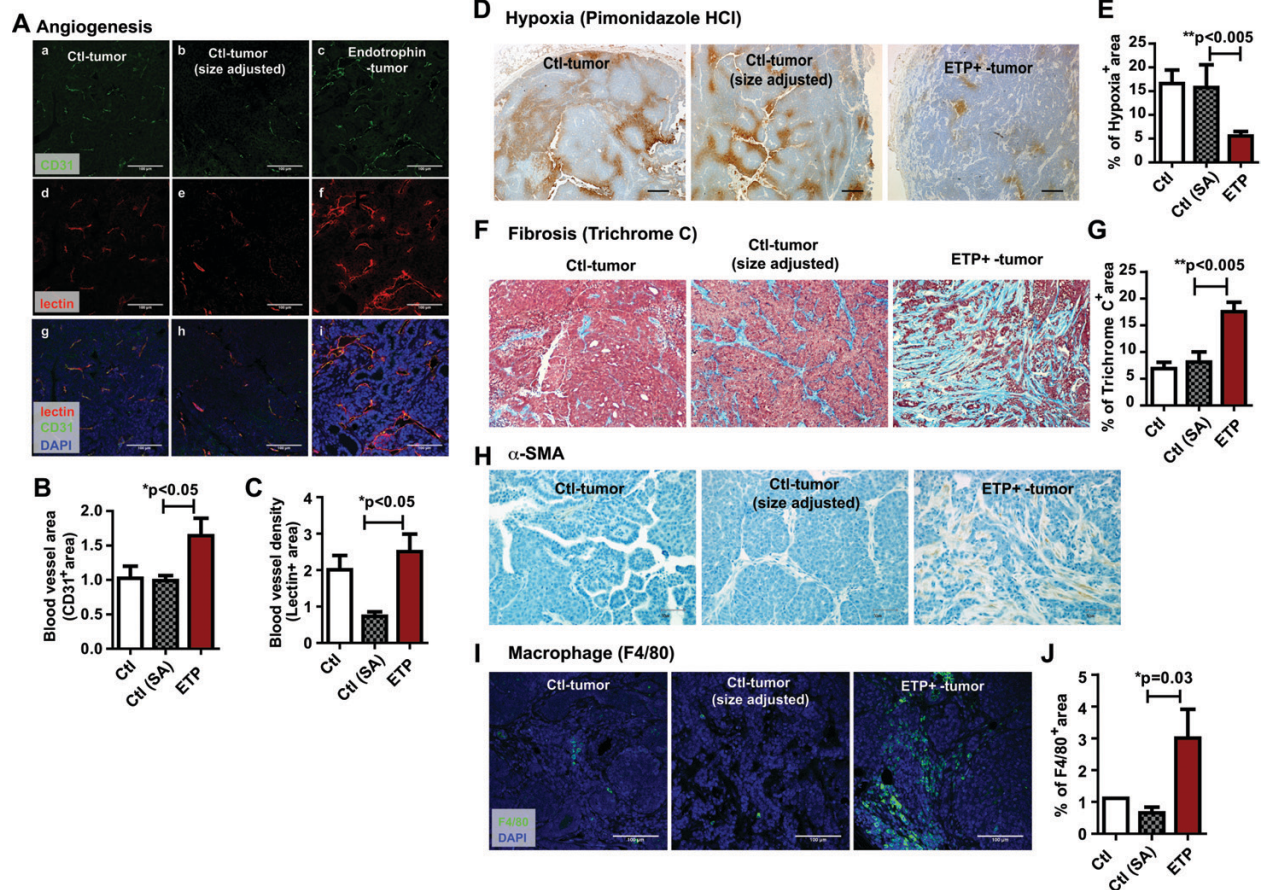


**Figure S8. Endotrophin augments tumor angiogenesis, fibrosis and inflammation through mediating tumor-stromal interactions.** Small pieces of tumor tissues derived from 12-week-old PyMT (Ctrl-tumor) and PyMT/endotrophin (ETP<sup>+</sup>-tumor) were implanted into the left or right side of a fat pad of a WT recipient, respectively. **A-C.** Angiogenesis is significantly increased in ETP<sup>+</sup>-tumors. Blood vessel area was determined by immunostaining with CD31; Functional vessel area was determined by lectin perfusion for Ctrl-tumors, tumor size adjusted Ctrl (SA)-tumors and ETP<sup>+</sup>-tumors. DAPI (nucleus) was co-stained. Scale bars: 100  $\mu$ m. CD31<sup>+</sup> area for blood vessel area (**B**) and functional vessel area (**C**) were quantified and represented as mean  $\pm$  SEM (5 independent images, n=5/ group). \*p<0.05 vs. Ctrl (SA)-tumor by *unpaired t-test*. **D-E.** Hypoxia regions were determined with a hypoxia probe (pimonidazole-HCL). Quantified results are represented as mean  $\pm$  SEM. \*\*p<0.005 vs. Ctrl (SA)-tumor by *unpaired t-test*. **F-G.** Fibrosis indices were determined by Masson's Trichrome C stain. Scale bars: 50  $\mu$ m. Quantified results are represented as mean  $\pm$  SEM. \*\*p<0.005 vs. Ctrl (SA)-tumor by *unpaired t-test*. **H.** Immunostaining for  $\alpha$ -SMA<sup>+</sup> myofibroblasts. **I-J.** Immunostaining for F4/80<sup>+</sup> macrophages. DAPI (nucleus) was co-stained. Scale bars: 100  $\mu$ m. Quantified results are represented as mean  $\pm$  SEM. \*p=0.03 vs. Ctrl (SA)-tumor by *unpaired t-test*.



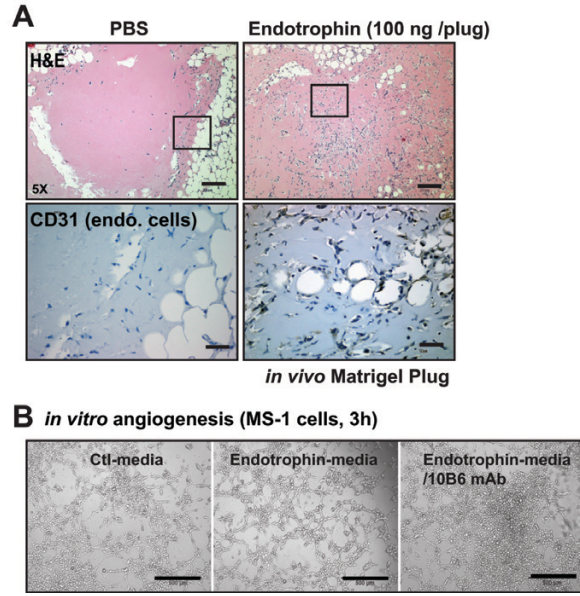


**Figure S9. Endotrophin effects on endothelial cell migration.** **A.** *in vivo* Matrigel bioassays were performed as described in Figure 6J. Matrigel plugs were analyzed by H&E and immunostaining for CD31 (endothelial cell marker). Scale bars: 200  $\mu$ m (H&E), and 50  $\mu$ m (CD31). **B.** *in vitro* Angiogenesis assay. MS-1 cells ( $5 \times 10^4$  cells/well) were plated in triplicate on the matrigel coated 12-well plates. Tubule formation was assessed 3 hours after incubation with conditioned media derived from H293 or H293-endotrophin overexpressing cells in the presence or absence of 10B6 (10  $\mu$ g/well). Scale bars: 500  $\mu$ m.

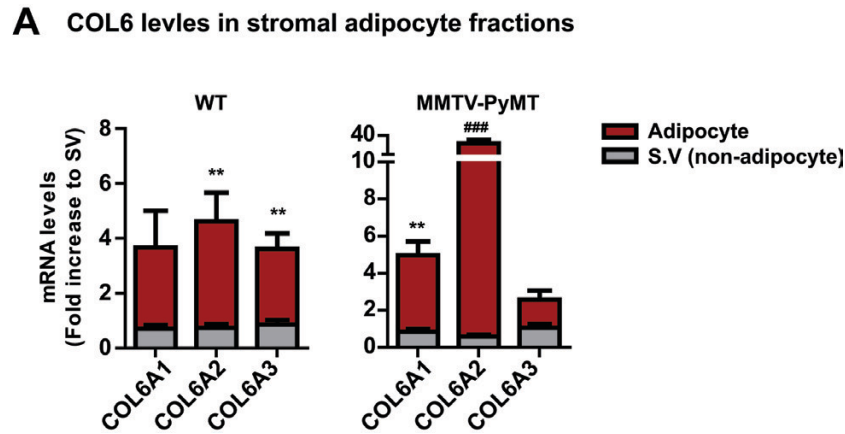


**Figure S10. Contributions of stromal adipocytes to COL6 mRNA expressions.** COL6A1-, A2 and -A3 mRNA levels in adipocytes (Adi) and stromal-vascular (S.V.) fractions in mammary glands for WT and PyMT mice. mRNA levels were determined by RT-qPCR. Results were normalized to  $\beta$ -actin and represented as mean  $\pm$  SEM. Bar graph is represented as -fold increase over the S.V. fraction. \*\* $p < 0.01$ , ### $p < 0.001$  vs. S.V. by *unpaired student t-test*. (n=4/group, tissues from 3 mice were pooled in one sample; i.e., total 12 mice/ group).

## Supplemental Methods

### *Mice*

COL6 knockout (COL6<sup>-/-</sup>) mice were generated as previously described by Bonaldo and colleagues (20). Endotrophin transgenic mice were generated by fusing cDNA encoding the mouse COL6A3-C5 domain (amino acids 2590-2657, NP\_034056) to the prolactin signal sequence at the amino-terminus (ATGGACAGCAAAGGTTTCGTCGCAGAAAGGGTCCCGCCTGCTCCTGCTGCTGGTGGTGTCAAATCTACTCTTGTGCCAGGGTGTGGTCTCC), which allows endotrophin to be secreted from the cells, into a plasmid containing the 3.2-kb MMTV (mouse mammary tumor virus) promoter and 3'-SV40 region. Transgene-positive offspring were genotyped using PCR with the following primer set: 5'-ACGAGAACAGATTCCACTCC-3' and 5'-TCAGCAGTAGCCTCATCATCAC-3'. Infrared fluorescent protein FP635 transgenic mice were generated by subcloning the FP635 domain originated from plasmid pTurboFP635 (Evrogen) into a plasmid containing the 3.2-Kb MMTV promoter and a conventional 3'-UTR region. Genotyping was performed using PCR with following primer set: 5'-AGAGACCTACGTCGAGCAGC-3' and 5'-GGGTCCATGGTGATACAAGG-3'.

### *Reagents*

Primary antibodies used in histological analysis: rabbit polyclonal against holo-COL6 (Abcam, Ab6588), CD31 (Abcam, ab38364),  $\alpha$ -smooth muscle actin (Abcam, ab5694), FSP1 (Abcam, ab27957), Vimentin (Cell Signaling, #5741) and E-cadherin (Cell Signaling, #3195); mouse monoclonal F4/80 (invitrogen, MF48000) and cytokeratin (Cell Signaling, #4545); rat monoclonal Ki67 (Dako Cytomation) and endomucin (Santa Cruz, sc-65495). TGF $\beta$  neutralizing antibody, 1D11 was generously providing by Dr. Rolf Brekken (UTSW Medical Center, Dallas).

### *Analysis of tumor progression and lung metastasis*

Tumor onset was monitored twice weekly by palpation. Tumor sizes were measured with a digital caliper twice weekly and the volumes were calculated as (length  $\times$  width<sup>2</sup>)/2. Inguinal tumors were weighted to determine tumor burden. Animals were sacrificed when the tumor burden visibly affected the host or when the tumors reached the IACUC predetermined limit of 20 mm along one axis. Metastatic tumor growth was determined by histological analysis with H&E stained lung tissues.

### *Immunoblotting*

Cell lysates were harvested using NP-40 lysis buffer, supplemented with phenylmethylsulfonyl fluoride (PMSF, 1 mM), protease inhibitor (Roche) and phosphatase inhibitor (Roche). Protein samples were immunoblotted using standard methods. For the culture media, differentiated 3T3-L1 adipocytes and preadipocytes were serum starved in DMEM media. Following overnight incubation, media was harvested and filtered (Millipore, 0.45mm). The conditioned media was concentrated using centrifugal filters (Amicon Ultra, 3K) at 14,000 g for 40 min. Secreted ETP was detected using  $\alpha$ -mouse ETP polyclonal antibody compared to COL6 (Abcam, Ab6588). The primary antibodies were detected with secondary IgG-labeled with infrared dyes emitting at 700 and 800 nm and visualized on the Licor Odessey Infrared Scanner. The scanned results were analyzed using the Odessey v2.1 software (Licor Bioscience). The complete unedited blots for all Western blotting images in the main are shown in the Supplementary images.

### ***Involution***

8-week-old females were housed individually upon pregnancy. Immediately after birth of their littermates, litter sizes were standardized to 6 pups per mother in order to prevent inter-mouse mammary gland variation. Involution was initiated by the removal of pups after 10 days of suckling. Mammary glands were collected for fixation at 0, 2, 3, 5 days after forced weaning and stained with H&E.

### ***Assessment of reproduction***

8-week-old female mice (5-9 mice/ group) were mated with wild type males. Each female was monitored for resulting pregnancies. Litters were monitored for survival to weaning age.

### ***Microarrays***

Total RNA was extracted from tumor tissue from 12-week-old PyMT and PyMT/endotrophin (n=12/ group). Microarray experiments were performed by the UTSW microarray core facility. The Mouse Illumina Bead Array platform (47K array) (Illumina, Inc.) was used in this study. Gene lists and cluster analyses of the data sets were performed using Ingenuity Pathway Software (Ingenuity systems) and David Bioinformatics Resource (<http://david.abcc.ncifcrf.gov/>). Gene profiling data are available from GEO (<http://www.ncbi.nlm.nih.gov/geo>) under accession no. GSE39622.

### ***In vitro angiogenesis***

A total 300  $\mu$ l/well of growth factor reduced matrigel (BD biosciences) was plated into 12 well plates. MS-1 cells ( $5 \times 10^4$ ) were seeded and images were acquired 3-4 hours after incubation with the conditioned media indicated.

### ***Luciferase reporter assay***

Cell lysates were harvested and analyzed for luciferase reporter assays following the manufacturer's protocol (Applied Biosystems, The Dual-Light luminescent reporter gene assay). The pGL3-SBE reporter, pGL3- $\beta$ Gal and indicated ETP constructs; pRA-ctrl (empty vector), pRA-sETP (secretion form of ETP) and pRA-ETP (intracellular form of ETP) were transiently transfected into Met-1 cells. 1 day after transfection, TGF $\beta$  (5 ng / ml) with either 1D11 (5  $\mu$ g/ ml) or IgG (5  $\mu$ g/ ml) was added overnight. Total cell lysates were analyzed for luciferase activity.

# Figure 2B

Original Blots

IB:  $\alpha$ -ETP  $\alpha$ -COL6 (Ab6588)

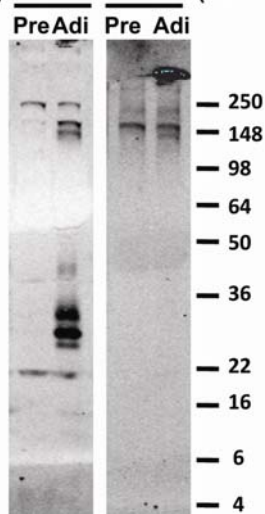


# Figure 7G

